

# Compressive Behavior of Fiber-Reinforced Honeycomb Cores

S. Rao\*, S. Banerjee, K. Jayaraman and D. Bhattacharyya

Centre for Advanced Composite Materials, Department of Mechanical Engineering, The University of Auckland, Auckland Mail Centre 1142, New Zealand. Phone: +64-9-3737599 Ext: 89050, Fax: +64-9-3737479, \*Email: srao006@aucklanduni.ac.nz.

**Abstract** Honeycomb core sandwich panels have found extensive applications particularly in the aerospace and naval industries. In view of the recent interest in alternative, yet strong and lightweight materials, honeycomb cores are manufactured from sisal fiber-reinforced polypropylene (PP) composites and the out-of-plane compressive behaviour of these cores is investigated. The cell wall material is modeled as a linear elastic, orthotropic plate/lamina and also as a linear elastic, quasi-isotropic material. The failure criteria for the reinforced honeycombs are theoretically developed. Failure maps that can be used for the optimal design of such honeycombs are constructed for a wide range of honeycomb densities. The results indicate a significant improvement in the load carrying capacity of the honeycomb cores after fiber reinforcement.

## Introduction

Honeycomb sandwich panels are being widely used in weight sensitive structural applications where high flexural rigidity is required. They are formed by bonding thin face sheets on either side of a low density honeycomb core. However, due to the high production costs, their application has been somewhat limited to aerospace and naval industries. To overcome this, low cost natural fibre-reinforced thermoplastics are now being used in the manufacturing of core materials for sandwich panels.

Honeycomb cores are commonly loaded in the out-of-plane direction as they exhibit excellent mechanical properties when loaded in that direction. Hence, the out-of-plane compressive behavior of honeycombs is of great importance. Research in this area is primarily concentrated in developing the relationship between the mechanical properties and the geometrical parameters of honeycombs. Extensive reviews of the mechanical properties of honeycomb materials can be found in the work of Gibson and Ashby [1]. The crushing behavior of metallic honeycombs under compressive loading was studied by Wierzbicki [2] which was a

modification of McFarland's work [3]. Zhang and Ashby [4] developed expressions for the failure loads of honeycombs under transverse compression and shear loading, that agree well with the experimental data for aramid paper honeycombs. In a recent study, Banerjee et al. [5] have developed a general methodology for optimizing the specific out-of-plane shear strength of reinforced honeycomb cores.

The current work focuses on recycled sisal fiber-reinforced polypropylene (PP) honeycombs. The manufacturing issues of these novel reinforced honeycombs are discussed first. The compressive behavior of honeycombs when subjected to out-of-plane compressive loading is investigated next. The failure criteria for reinforced honeycombs are theoretically developed and failure maps are constructed for a wide range of honeycomb densities. The improvement in the load carrying capacity of reinforced honeycombs as compared to that of unreinforced honeycombs is explained quantitatively. Experimental data of the manufactured honeycombs are compared with the theoretical predictions.

## Honeycomb core manufacturing

The honeycombs were manufactured from extruded sisal-polypropylene composite sheets. The composite is made of sisal fibers of lengths 1-3 mm and aspect ratio  $\sim 30$ . Its tensile modulus is 4-9 GPa and tensile strength is 500-800 MPa. The base matrix PP has a tensile modulus of 0.9-1.2 GPa and a tensile strength of 33 MPa.

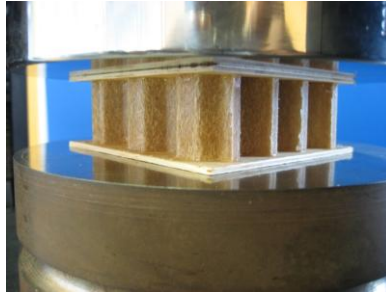


**Fig. 1** Honeycomb core sandwich panel manufactured from sisal-PP composite.

The sheets were manufactured from recycled sisal-PP pellets in a twin screw extruder through a die with 300 mm x 2.5 mm rectangular cross-section and were calendered to 1.5 mm thickness, with a fiber volume fraction of  $\sim 0.24$ . The extrusion process aligned the fibers more or less in the flow direction, making the

material mildly orthotropic in nature. The extruded sheets were thermoformed between matched-dies to obtain profiled panels; these formed panels were assembled and bonded with adhesives to obtain hexagonal honeycombs, Fig.1. The honeycombs were manufactured in such a way that the fibres in the cell walls were aligned in the loading direction, so that it can produce best performance under compressive loading. Tests were performed on the composite sheets (cell wall material) and honeycomb cores as per ASTM standards. The mechanical properties of the sheet material and the honeycomb cores are shown in Table 1.

**Table 1.** Mechanical properties of the composite sheet material and the honeycomb cores

Material property		Value	Test standard
Tensile strength	Longitudinal $\sigma_{11}$	36.40 MPa	ASTM D 638
	Transverse $\sigma_{22}$	21.40 MPa	ASTM D 638
Tensile modulus	Longitudinal $E_{11}$	3.87 GPa	ASTM D 638
	Transverse $E_{22}$	2.17 GPa	ASTM D 638
Poisson's ratio	Major $\nu_{12}$	0.40	ASTM D 638
	Minor $\nu_{21}$	0.20	ASTM D 638
Shear modulus $G_{12}$		2.87 GPa	ASTM D 4255
Shear modulus $G_{13}=G_{23}$		157.48 MPa	ASTM D 732
Sheet compressive strength		71.20 MPa	Modified ASTM D 695
Sheet compressive modulus		3.50 GPa	Modified ASTM D 695
Core compressive strength		8.73 MPa	ASTM C 365
Core compressive modulus		268.9 MPa	ASTM C 365
Sheet density		960 kg/m <sup>3</sup>	-
Core density		156 kg/m <sup>3</sup>	-

## Out-of-plane compressive behavior of reinforced honeycombs

A typical hexagonal cell and the associated geometrical parameters are shown in Fig. 2 (a), where,  $h/l$ ,  $\theta$ ,  $t_1/l$  and  $t_2/t_1$  are the non-dimensional parameters that define the geometry of a hexagonal cell [1]. Fig. 2 (b) shows a unit cell made of three cell walls of half length connected at a node.  $H$  is the height of a cell, perpendicular to the plane of the paper. The unit cell shown in Fig. 2(b) has an area of  $(h+l\sin\theta)l\cos\theta$ , considering the periodicity and the symmetry of the honeycomb structure. The relative density  $\phi$  of a low density hexagonal honeycomb can be approximately expressed as [5]

$$\phi = \frac{\rho^*}{\rho} = \frac{t_1}{l} \frac{(h/l)(t_2/t_1) + 2}{2(h/l + \sin\theta)\cos\theta} \quad (1)$$

where,  $\rho^*$  and  $\rho$  are the densities of the honeycomb and the cell wall material, respectively.

The possible failure mechanisms for thermoplastic honeycombs subjected to out-of-plane compressive force can be identified as elastic buckling of the cell walls, fracture of the cell wall material and de-bonding of the double thickness cell walls.

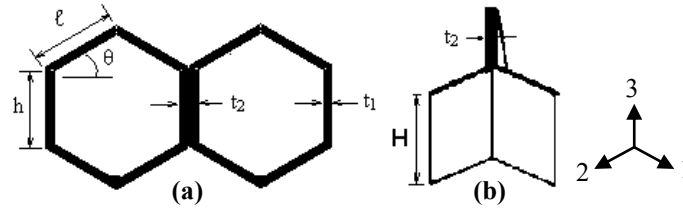


Fig. 2 Typical hexagonal cells showing (a) the associated geometrical parameters and (b) unit cell.

Because of the manufacturing process involved, the cell wall material is mildly orthotropic. In addition, the principal material direction (stiffer direction) is oriented in the depth direction of the honeycomb, i.e. 3 direction, perpendicular to the paper. Therefore, the cell wall material is modeled here as a linear elastic specially orthotropic plate/lamina under plane stress condition and also as a quasi-isotropic material, neglecting the mild orthotropy (as the degree of orthotropy  $\approx 2$ ). The failure loads are evaluated for the compressive loading applied on the unit cell in the 3 direction. For uniform compression of the cell walls, each wall carries an equal amount of compressive stress  $\sigma_{33}$ . Considering the force equilibrium in the 3 direction, the relationship between the external stress  $\sigma_{33}^*$  and  $\sigma_{33}$  can be expressed as

$$\sigma_{33}^*(h + l \sin\theta)l \cos\theta = \sigma_{33}t_2 \frac{h}{2} + 2\sigma_{33}t_1 \frac{l}{2} \quad (2)$$

and by using (1),

$$\sigma_{33}^* = \sigma_{33}\phi \quad (3)$$

is obtained in the same form as in [4]. Therefore, the compressive stress in the cell wall is inversely proportional to the relative density of the honeycomb. The failure

criteria is now developed for a honeycomb made of regular hexagonal cells with  $h/\ell = 1$ ,  $\theta = 30^\circ$ ,  $t_2/t_1 = 2$ ,  $t_1 = t$  and hence,  $\phi = \frac{8}{3\sqrt{3}} \frac{t}{l}$ .

The elastic buckling load of the cell walls under compressive loading is now calculated, applying relevant boundary conditions. If all the edges are assumed to be simply supported, the lower bound of the critical buckling load is obtained, whereas the assumption of fixed edges predicts the upper bound. In reality, as cell walls are restrained by their neighbors at the edges and by the skins at the top and bottom, the edges between the core and skins may be considered fixed, but the fixity in the remaining edges is somewhere in between the simply supported and fixed. Hence, in this work, all the edges are assumed to be simply supported and thus, the lower bound of the critical buckling load is calculated. The lowest buckling load  $P_{cr}$  for a single specially orthotropic lamina (per unit width) under compression, with no extension-bending coupling, can be expressed as [6]

$$P_{cr} = \left( \frac{\pi^2 D_{22}}{l^2} \right) \left[ \left( \frac{D_{11}}{D_{22}} \right) (l/H)^2 + 2 \left( \frac{D_{12} + 2D_{66}}{D_{22}} \right) + (H/l)^2 \right] \quad (4)$$

where,  $D_{ij} = Q_{ij}t^3/12$  are the typical bending stiffnesses of the cell wall, expressed in terms of the these stiffnesses  $Q_{ij}$  of the cell walls and  $i, j = 1, 2, 6$ .

Cell wall buckling is governed by the bending of the cell wall and hence, the buckling stress is proportional to  $(t/\ell)^3$ . Therefore, although the cell walls carry equal stresses, the buckling load for the double thickness (2t) cell wall is eight times higher than that of the inclined member (t). Hence, the inclined members buckle first and eventually, the double thickness cell walls buckle due to a loss of restraint at the edges. Therefore, neglecting post buckling, the critical applied stress for the honeycomb can be calculated considering the buckling of the inclined members, from equations (3) and (4),

$$\begin{aligned} \sigma_{cr33}^* &= (\pi^2 Q_{22}) \frac{2}{9\sqrt{3}} \frac{t^3}{l^3} \left[ \left( \frac{D_{11}}{D_{22}} \right) (l/H)^2 + 2 \left( \frac{D_{12} + 2D_{66}}{D_{22}} \right) + (H/l)^2 \right] \\ &= (\pi^2 Q_{22}) \frac{9}{256} \phi^3 \left[ \left( \frac{D_{11}}{D_{22}} \right) (l/H)^2 + 2 \left( \frac{D_{12} + 2D_{66}}{D_{22}} \right) + (H/l)^2 \right] \end{aligned} \quad (5)$$

If the cell wall is assumed as a quasi-isotropic material with  $E = E_{11}$  and  $\nu = \nu_{12}$ , then using Euler's formula for elastic buckling load of a plate (per unit width) under compression [7],  $P_{cr} = K\pi^2 E t^3 / 12 \ell^2 (1-\nu^2)$ , the critical buckling load for the honeycomb can be expressed using (3),

$$\sigma_{cr33}^* = \frac{2}{9\sqrt{3}} \frac{K\pi^2 E t^3}{1-\nu^2} = \frac{9}{256} \frac{K\pi^2 E}{1-\nu^2} \phi^3 \quad (6)$$

where the factor K represents the end conditions of the cell wall and also depends on the ratio of  $H/\ell$ .

When the compressive stress in the cell walls reach the fracture stress of the cell wall material  $\sigma_{33\max}$ , cell walls fracture and causes the honeycomb failure. The corresponding external load is the critical fracture load for the honeycomb core and is given by

$$\sigma_{33}^* = \sigma_{33\max} \phi \quad (7)$$

## Results and discussion

The failure maps for reinforced honeycombs under compressive loading are shown in Fig. 3. The plot shows the maximum load carrying capacity of honeycombs as a function of the relative density and  $t/l$  ratio, based on orthotropic and quasi-isotropic assumptions. For convenience, all the stress values are normalized with respect to  $E_{11}$ . The critical buckling load varies with the core depth and cell wall length ratio (refer (5) and (6)). The buckling load is plotted here for a core depth of 25 mm as a reference for which the laboratory experiments were performed. The value of  $K$  is taken as 4.02 for the isotropic case [7]. The ultimate compressive strength of the honeycomb is calculated using (7) on the basis of the average experimental value of compressive strength of the cell wall material which is 71.2 MPa, refer Table 1. The map shows that the buckling load prediction based on the orthotropic assumption is higher than that based on the quasi-isotropic assumption. The failure modes will now be described with reference to the orthotropic case and that is applicable for the quasi-isotropic case as well.

Fig. 3 (a) shows that when the honeycomb relative density is lower than the intersection point (P) of the two curves, honeycomb failure is governed by cell wall buckling. The density corresponding to point P indicates the occurrence of simultaneous buckling and fracture of the cell walls and indicates the balanced relative density for this material. With any further increase in the relative density beyond this point, the dominant failure mode changes from buckling to fracture of cell walls. The transition load at which the two modes of failure occur simultaneously, can be calculated by equating  $\sigma_{33}^*$  from (5) and (7), and eliminating  $\phi$ . In the present example, the load index is calculated as  $1.5 \times 10^{-3}$ , which corresponds to 5.87 MPa; the associated relative density is about 0.08.

The honeycomb load capacities are plotted in Fig. 3 (b) for various  $t/l$  ratios. For the critical load index  $7.78 \times 10^{-4}$ ,  $t/l$  ratio is 0.042 for the relative density of 0.065. Cell wall buckling is governed by the bending of the cell wall and hence, is proportional to  $(t/l)^3$ , refer Eq. (6). On the other hand, fracture resistance factor is  $t/l$ , Eq. (7). Hence, with increasing honeycomb density  $\phi$  and hence,  $t/l$  ratio, effective buckling resistance increases at a much higher rate than the resistance to fracture. As a result, cell walls become more prone to failure by fracture. Therefore, a change in the failure mode is observed when the relative density approaches a certain critical value (point P), as shown in Fig. 3. The failure map can also be

used for designing the honeycomb density and geometrical parameters for a certain prescribed loading.

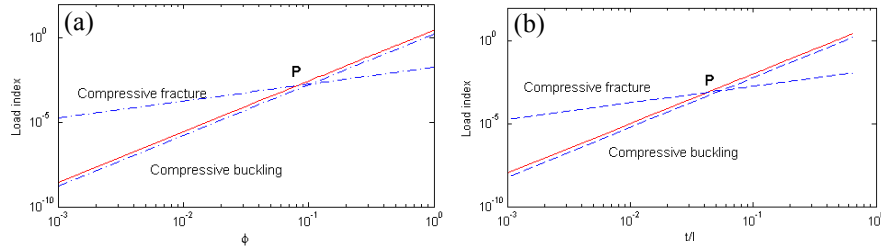


**Fig. 3** Failure maps for reinforced honeycomb: (a) load index with respect to relative density  $\phi$  and (b) load index with respect to  $(t/l)$  ratio. Legend: — indicates orthotropic case and -- indicates quasi-isotropic case.

### ***Quantitative comparisons of strength between the reinforced and un-reinforced honeycombs***

For the *buckling* mode of failure, comparison of the expressions for the reinforced and un-reinforced cases, Eq. (6), show that for the same relative density, the ratio of the load carrying capacity of the reinforced PP honeycomb to that of the PP honeycomb is given by the ratio of the Young's modulus of the respective cell wall material,  $E^r/E$ , where superscript 'r' denotes the reinforced case. The cell wall buckling resistance improves with the increase in the Young's modulus of the cell wall material, and this, in turn, improves the load capacity of reinforced PP honeycomb. However, the addition of reinforcements would increase or decrease the density of the cell wall material depending upon whether the reinforcing fiber is of high or low density as compared to the base material itself. If a low density fiber is used, then the density of the composite is reduced and it offers an added advantage.

From Eq. (6), the ratio of the load carrying capacity of the reinforced honeycomb and the base honeycomb of same densities is in the ratio of its specific stiffnesses ( $E/\rho$ ) of the respective cell wall materials, multiplied by  $(\rho/\rho^r)^2$ . In this work,  $E^r/E$  is 387%, and the increase in density is from 900 to 960  $\text{kg/m}^3$ , by  $\sim 6.67\%$ . Hence, the overall improvement in the load carrying capacity of the reinforced honeycomb to that of the PP honeycomb of the same density is about  $3.87 \times 0.82 = 3.17$ , i.e. 317%. Thus showing that, the increase in specific stiffness of cell wall material would result in an enhanced load carrying capacity of the honeycomb. On the other hand, for the same loading, relative density ratio of the reinforced and unreinforced honeycomb can be obtained using Eq. (6) as  $\sqrt[3]{E^r/E} = 0.64$ , i.e. the relative density reduction is about 36%. The reduction is

less now because the relative density is proportional to the cube root of the respective moduli. The overall reduction in honeycomb density after taking into account the effect of the reinforcement ( $\rho/\rho^r$ ) is about  $0.64 \times 1.07 = 0.68$ , or 32%.

For the *fracture* mode of failure, as seen from Eq. (7), improvement in the load carrying capacity of the reinforced honeycomb as compared to the un-reinforced case having the same relative density is in the ratio  $\sigma_{33\max}^r/\sigma_{33\max}$ . If the increase in density of the cell wall material is taken into account (same for both failure mechanisms), net improvement in strength for the same honeycomb density is in the ratio of the specific strengths ( $\sigma_{33\max}/\rho$ ) of the corresponding cell wall materials. In the current work, the ratio is  $\sigma_{33\max}^r/\sigma_{33\max} = 2.16$  and therefore, improvement in strength is 216% for the reinforced honeycomb. Taking into account of the effect of density, load carrying capacity of the reinforced honeycomb improves by  $2.16 \times 0.94 = 2.02$ , i.e. 202%.

### ***Comparison of theory with experimental result***

The average compressive strength of these honeycombs was measured as 8.73 MPa; corresponding relative density is 0.16. Theoretical calculations indicate that the dominant failure mode of these honeycombs is cell wall fracture with the value of  $\sigma_{33}^*$  as 11.39 MPa. Observation of the real honeycomb specimens indicates that cell wall buckling is the dominant mode of failure. Fig. 3 indicates that the buckling strengths of the honeycomb based on the orthotropic and quasi-isotropic assumptions to be 44.45 MPa and 26.39 MPa, respectively. Therefore, both the assumptions indicate higher buckling load as compared to the experimental value, with the quasi-isotropic assumption predicting lower load of the two. In the buckling load calculation, shear deformation of the cell wall is neglected. As the  $t/\ell$  ratio of the cell wall is about 6, including the shear deformation of the cell wall would reduce the buckling load. In addition, the cell wall material can have elastic-plastic buckling, that can cause buckling at a lower load. Any imperfection/damage in real honeycomb can also reduce the buckling load considerably. Hence, the elastic buckling load calculated here can be considered as the upper bound. With the reduction in buckling load, the intersection point (P) would move further right and thus honeycombs with a wide range of densities would fail by buckling instead of fracture. Hence, the correlation with the experiments would improve, especially for higher densities. In future, the cell wall will be modeled as an elastic-plastic material for an improved prediction of the buckling load. Further research is in progress in this area.

## Concluding remarks

With an aim to produce low cost yet stiff and strong core materials, honeycombs were manufactured by a matched die forming process using recycled sisal fibre-reinforced PP sheets. The out-of-plane compressive behaviour of these honeycomb cores was investigated and the failure loads were evaluated. Failure maps that can be used for optimal design of the cell geometry of honeycombs were constructed. The short fibre-reinforcement in the cell walls is found to have significantly increased the load carrying capacity of the fibre-reinforced honeycomb cores.

**Acknowledgments** The authors would like to thank the BioPolymer Network (BPN) and the Foundation for Research Science and Technology, New Zealand for their funding of this research.

## References

- [1] Gibson LJ and Ashby MF (1997) Cellular Solids: Structure and Properties. Cambridge Univ. Press, Cambridge.
- [2] Wierzbicki T and Abramowicz W (1983) On the crushing mechanics of thin-walled structures. *J. Appl. Mech. ASME*, 50(4A):727-734.
- [3] McFarland RK (1963) Hexagonal cell structures under post-buckling axial load. *AIAA J* 1(6):1380-1385.
- [4] Zhang J and Ashby MF (1992) The out-of-plane properties of honeycombs. *Int. J. Mech. Sci* 34(6):475-489.
- [5] Banerjee S, Battley M and Bhattacharyya D (2008), *Mech. Adv. Mat. Str.*, in press.
- [6] Reddy JN (2004) *Mechanics of Laminated Composite Plates and Shells Theory and Analysis*. CRC Press, Boca Raton.
- [7] Timoshenko SP and Gere JM (1961) *Theory of Elastic Stability*. McGraw-Hill Book Company, New York.